Primljen / Received: 10.12.2021.
Ispravljen / Corrected: 22.7.2022.
Prihvaćen / Accepted: 12.8.2022.
Dostupno online / Available online: 10.11.2022.

# Glass fiber reinforced ultra-high strength concrete with silica fume

Authors:

Assist.Prof. **Sathyakumar Natarajan**
Bannari Amman Institute of Technology
Department of Civil Engineering
Tamilnadu, India
sathyakumarn@bitsathy.ac.in
**Corresponding author**

Assoc.Prof. **Arun Murugesan**, PhD. CE
PSG Institute of Technology and Applied Research
Department of Civil Engineering
Tamilnadu, India
arun@psgitech.ac.in

Prof. **Jagatheeswaran Dhanapal**, PhD. CE
Sona College of Technology, Tamilnadu, India
Department of Civil Engineering
profdjpillai@gmail.com

Prof. **Arunachalam Narayanan**, PhD. CE
Bannari Amman Institute of Technology
Department of Civil Engineering
Tamilnadu, India
arunachalamn@bitsathy.ac.in

Research Paper

Sathyakumar Natarajan, Arun Murugesan, Jagatheeswaran Dhanapal, Arunachalam Narayanan

**Glass fiber reinforced ultra-high strength concrete with silica fume**

Conventional glass fiber-reinforced concrete (GFRC) has wide applications in high-rise buildings, bridges, and renovation works. In this study, ultra-high-strength glass fiber reinforced concrete (UHS-GFRC) mixtures were developed to minimize the size of the structural members. The percentage of glass fiber was varied as 0%, 0.03%, 0.06%, 0.09%, and 0.12%. In this investigation, ten beams were cast and tested, with two span-to-effective-depth (a/d) ratios of 1.6 and 2. All the tested specimens attained their respective strengths; however, the strength values varied. Specifically, the specimens reinforced with 0.09% and 0.06% of glass fiber exhibited the highest flexural and shear strengths, respectively. The results obtained in this study can be utilized to select optimum mixtures of UHS-GFRC under satisfying service conditions.

**Key words:**

**ultra-high strength concrete, fiber reinforced concrete, silica fume, glass fiber, shear failure, flexural failure**

Prethodno priopćenje

Sathyakumar Natarajan, Arun Murugesan, Jagatheeswaran Dhanapal, Arunachalam Narayanan

**Beton ultravisoke čvrstoće pojačan staklenim vlaknima sa silicijskom prašinom**

Konvencionalni beton pojačan staklenim vlaknima (GFRC) ima široku primjenu u visokim zgradama, mostovima i radovima obnove. U ovom istraživanju razvijene su mješavine betona pojačanog staklenim vlaknima ultravisoke čvrstoće kako bi se smanjila veličina nosivih elemenata. Varijacija postotka staklenih vlakana bila je 0 %, 0,03 %, 0,06 %, 0,09 % i 0,12 %. U ovom istraživanju izrađeno je i ispitano deset greda, s dva omjera raspona i statičke visine (a/d) od 1,6 i 2. Svi testirani uzorci opterećeni su do sloma, no vrijednosti čvrstoće su varirale. Točnije, uzorci pojačani s 0,09 i 0,06-postotnim staklenim vlaknima pokazali su najveću savojnu i posmičnu čvrstoću. Rezultati dobiveni ovim istraživanjem mogu se iskoristiti za odabir optimalnih mješavina betona ultravisoke čvrstoće pojačanog staklenim vlaknima u zadovoljavajućim radnim uvjetima.

**Ključne riječi:**

**beton ultravisoke čvrstoće, beton pojačan vlaknima, silicijska prašina, staklena vlakna, lom posmikom, lom savijanjem**

## 1. Introduction

Currently, the application of high-strength concrete (HSC) is inevitable. Many studies have been conducted on high-strength concrete, normally produced by adding GGBS, fly ash with high fiber content, or by some special curing methods; thus, increasing the cost of construction and cannot be implemented in the construction field. Therefore, this experimental research aims to identify the optimum percentage of glass fiber for improving mechanical behavior in a cost-effective manner. The concrete mixes of M20, M30, M40, and M60 grades with a constant percentage of glass fiber of 0.03 % and without glass fiber concrete specimen mixes show 10 to 20 % incremental strength when compared to conventional concrete for 28 days [1]. The various percentages of glass fibers of 0, 0.02, 0.04, and 0.06 % for both M20 and M30 grades of concrete specimens with alkali-resistant glass fibers significantly improve the mechanical properties irrespective of the workable property of the concrete mix, and the strength increase percentage for a higher grade of concrete is marginally high [2].

Developing ultra-high-strength concrete (UHSC) using local materials, such as fine sand, cement, quartz powder, micro silica, and steel fibers with different mix proportions increases the mechanical properties; thus, the UHSC and compressive strength of UHSC with fiber is greater than the compressive strength of plain concrete. The flexural strength of UHSC with steel fibers is 68 % greater than UHSC without steel fibers [3]. Manufactured sand has been used partially to replace natural sand, cement, fly ash, silica fume, coarse aggregate (12.5 mm), and superplasticizer with water. In addition, it has shown improved mechanical properties. The flexural strength increases with the addition of M-sand and a mix of 10 % silica fume [4].

Compressive strength was improved for a mixture of silica fume and glass powder instead of 100 % of silica fume being replaced by glass powder [5].

Concrete with a compressive strength of 100 MPa to 200 MPa is called UHSC and has a low water-binder ratio and high binder content [6]. Manufactured sand is used more owing to the limiting resources of natural sand availability, Portland pozzolana cement of 53 grade, M-sand as fine aggregate, coarse aggregate, water, and the superabsorbent polymer for the control mix as a self-curing membrane compound, considering a compressive strength of 20 MPa; however, the workability of the concrete is reduced for M-sand as compared to that of natural sand. Membrane and self-curing yield superior results compared with air and standard moist curing [7].

Adding silica fume with other constituents increases the flowability and mechanical properties of UHSC and decreases the heat of hydration [8]. An investigation has been conducted on the effect of high temperature on UHSC with polypropylene (PP) and nylon (NY) fibers, which shows spalling of concrete is controlled by the addition of 0.15 % to 0.25 % of fibers [9].

A study was conducted on the effect of nano-silica on the autogenous shrinkage, hydration, and compressive strength of UHSC. Owing to the large specific area of nS, the amount of superplasticizer increases with increasing nS content. Isothermal calorimetric data show that the setting time delays the addition of the polycarboxylate superplasticizer. The variable-temperature hydration value decreases, and the maximum internal temperature decreases as the amount of nS increases. XRD analysis shows that CH intensity decreases in UHSC with nS (2 % and 4 %) owing to the consumption of CH by nS. As the addition of nS increases, the ability to enhance the compressive strength of UHSC decreases because of the high surface energy of nS [10].

When the amount of silica fume increases to 22 %, the flowability increases; however, beyond 22 %, the flowability decreases. Total hydration of UHSC increases with the addition of 15 % of silica fume and decreases by 30 %. Owing to the high pozzolanic effect and fine particle size, silica fume positively affects the early compression strength. When the slag incorporated to reduce the C/S ratio is mixed alone, it decreases the compressive strength; however, when mixed with silica fume, it increases the compressive strength. With an increase in the amount of silica fume, the porosity of UHSC decreases, which may be owing to its filler effect and pozzolanic activity, in which more C-S-H gel is produced, reducing the pore size. The calcium hydroxide content decreases as the slag or silica fume content increases [11].

The reduction in the water-binder ratio increases the strength, resulting in water demand; thus, it is necessary to add a high water-reducing agent for compensation. Cement, silica fume, methacrylate ether-based PCE, and allyl ether-based PCE with different lengths (shorter trunk chain) are effective for UHSC production. The effective dispersion of silica fume is necessary to increase the flowability of the UHSC mix. Therefore, a blend with this PCE can achieve the best performance in UHSC. If the shape of the silica fume is irregular, PCE increases [12].

The recycled ceramic aggregate has more porosity than the aggregate used in gravel basalt ceramic aggregate concrete. The cement paste cannot fully enter the pores of the ceramic aggregate, and a small amount of air is closed in the aggregate grains. Thus, the ceramic-recycled aggregate can be used in the production of UHSC with compressive strength over 120 MPa and does not require any additional methods to utilize in UHSC production [13].

Therefore, in this experimental research, the mechanical behavior, flexural, shear strength, and behavior of ultra-high-strength glass fiber reinforced concrete (UHS-GFRC) beams with an optimum percentage of glass fiber and other constituents of concrete were examined in detail.

Table 1. Properties of cement, fine and coarse aggregate

| S.No. | Test conducted | Cement | Fine aggregate | Coarse aggregate |
|---|---|---|---|---|
| 1 | Normal consistency [%] | 26 | - | - |
| 2 | Initial setting time [minute] | 30 | - | - |
| 3 | Final setting time [minute] | 340 | - | - |
| 4 | Specific gravity | 3.1 | 2.64 | 2.78 |
| 5 | Water absorption [%] | - | 1.745 | 0.6 |
| 6 | Bulking [%] | - | 3.99 | - |
| 7 | Bulk density [kg/m$^3$] | - | 3885.45 | - |
| 8 | Fineness modulus | - | 2.97 | 9.2 |
| 9 | Impact value [%] | - | - | 4.86 |
| 10 | Crushing value [N/mm$^2$] | - | - | 2.5 |
| 11 | Abrasion value [%] | - | - | 4.12 |

Table 2. Details of beams with glass fiber percentages

| S.No | Designation of Beams | Percentage of glass fiber added |
|---|---|---|
| 1 | Ultra-high strength concrete flexure beam (UHSCFB0) | 0 |
| 2 | Ultra-high strength concrete shear beam (UHSCSB0) | 0 |
| 3 | Ultra-high strength concrete flexure beam (UHSCFB1) | 0.03 |
| 4 | Ultra-high strength concrete shear beam (UHSCSB1) | 0.03 |
| 5 | Ultra-high strength concrete flexure beam (UHSCFB2) | 0.06 |
| 6 | Ultra-high strength concrete shear beam (UHSCSB2) | 0.06 |
| 7 | Ultra-high strength concrete flexure beam (UHSCFB3) | 0.09 |
| 8 | Ultra-high strength concrete shear beam (UHSCSB3) | 0.09 |
| 9 | Ultra-high strength concrete flexure beam (UHSCFB4) | 0.12 |
| 10 | Ultra-high strength concrete shear beam (UHSCSB4) | 0.12 |

## 2. Materials used and mix design

Ordinary Portland cement of grade 43, M-sand as a fine aggregate, and 12 mm coarse aggregates were used. Preliminary tests were performed to identify the properties of the materials used, with the results shown in Table 1.
Silica fume and Master glenium sky 8233 type superplasticizers were used as admixtures. Alkali-resistant glass fibers with a filament diameter of 14 microns, specific gravity of 2.68, and length of 12 mm were used in this investigation. Different percentage of glass fiber added with UHSC is shown in Table 2.
The properties of the steel bars used in this study are presented in Table 3.
The mix design focuses on developing the most economical UHSC mix. Optimum cement content was obtained in this study by conducting iterative studies for various trial mixes. The mix proportions are listed in Table 4.

Table 3. Properties of reinforced steel bar

| Diameter of bar [mm] | Percentage elongation [%] | Yield stress [N/mm$^2$] | Ultimate tensile stress [N/mm$^2$] | Young's modulus $E_s$ [N/mm$^2$] |
|---|---|---|---|---|
| 8 | 17.3 | 428.16 | 515.25 | $2.10 \cdot 10^5$ |
| 10 | 16.3 | 417.24 | 497.6 | $2.08 \cdot 10^5$ |

Table 4. Mix ratio for 1 m$^3$ of concrete

| Cement [kg] | Fine aggregate [kg] | Coarse aggregate [kg] | Silica fume [kg] | Superplasticizer [liters] | W/b ratio |
|---|---|---|---|---|---|
| 756 | 540 | 1080 | 75.6 | 10.8 | 166.32 |
| Mix proportions | | | | | |
| 1 | 0.714 | 1.429 | 0.1 | 0.0143 | 0.2 |

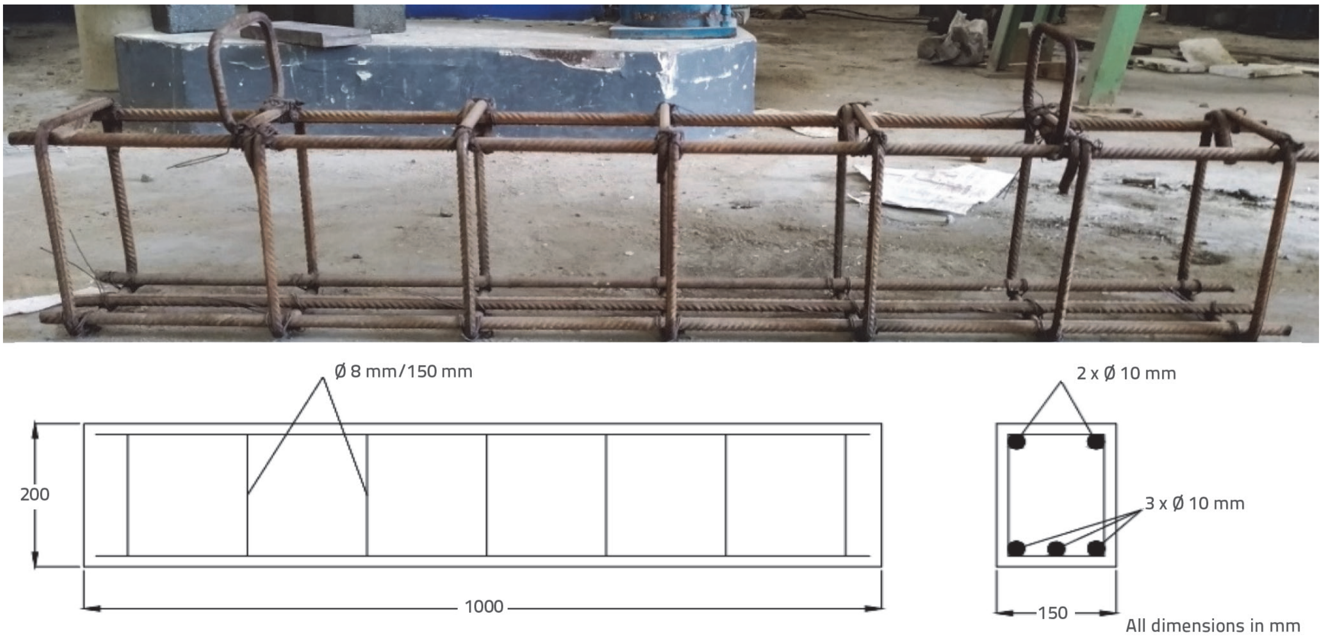


**Figure 1. Reinforced steel details**

## 3. Specimen details

A size of 1000 mm × 150 mm × 200 mm with an effective depth (d) of 170 mm was used for all beams in this investigation. Three 10 mm diameter bars as longitudinal bars, two 10 mm diameter bars as hanger bars, and two-legged 8 mm diameter bars at 150 mm center to center spacing as transverse reinforcement ($A_{sv}$) were used, as shown in Figure 1. The same reinforcement ratio was used for all the beams.

After the mold was assembled, the steel reinforcement was placed inside the mold on cover blocks of thickness 25 mm. A pan mixer was used to mix the materials. First, the cement, silica fume, and M-sand were thoroughly mixed until a uniform mix was obtained in the concrete mixer. Thereafter, coarse aggregate and glass fiber were added to this mix. Finally, a superplasticizer, along with water, was added to obtain a uniform mix. Thereafter, the concrete mixture was poured into the mold of the beam and companion specimens and then compacted using a needle vibrator. The specimens were subjected to immersion curing. The casting and curing of the specimens in the tank are shown in Figure 2. Ten beams were cast along with companion specimens to study the behavior and strength of UHS-GFRC beams in flexure and shear. All the beams were divided into two groups to test for flexure and shear with span-to-effective depth ratios (a/d) of 2 and 1.6, respectively.

## 4. Experimental setup and Instrumentation

Compressive strength, split tensile strength, and flexural strength tests were performed according to codes IS 516:1959, IS 5816:1999, and IS 9399:1979, respectively, to investigate

**Figure 2. Casting of beam, companion specimens and curing of specimens**

the mechanical properties of UHS-GFC. The grids were marked with 50 mm spacing on all the beams and were used to assist in drawing the crack patterns and measuring the widths of the cracks at the required locations. The beams were tested in a 750 kN capacity loading frame. The load was applied using a hydraulic jack of 500 kN capacity and distributed as two concentrated loads on the beam. The central load was measured using a proving ring of 200 kN capacity. The span-to-effective depth ratios (a/d) were maintained at 2 and 1.6. Deflections were measured at mid-span, quarter-span, and 3/4$^{th}$ span points using linear variable displacement transducers (LVDT). The deflection, crack width, and crack pattern were recorded at each loading increment.

## 5. Results and discussions

### 5.1. Compressive strength

Fifteen cubes with sizes of 100 mm × 100 mm × 100 mm were cast for different percentages of glass fiber to investigate the compressive strength. We found that the compressive strength of the UHSC mixtures obtained for all mixes was greater than 130 N/mm$^2$. While adding 0.03 % of glass fiber to the mix, the compressive strength increased by 1.22 %, and further increased strength by 0.82 % with 0.06 % of glass fiber. Furthermore, 0.09 % of glass fiber content in the mix showed a 1.15 % increase in strength, and a further increased strength of 1.73 % when 0.12 % of glass fiber was added. The results showed that the increase in fiber content was directly proportional to the compressive strength up to an optimum percentage; however, the strength variation was approximately 1 %. Based on these compressive strength test results, as shown in Figure 3, the mix with and without glass fiber provides ultrahigh-strength concrete. The strength is improved by adding glass fiber to concrete [1]. This mix can be used to fabricate structural members in high-rise buildings by minimizing the size of the member compared with a conventional mix of concrete for the same load-carrying condition.

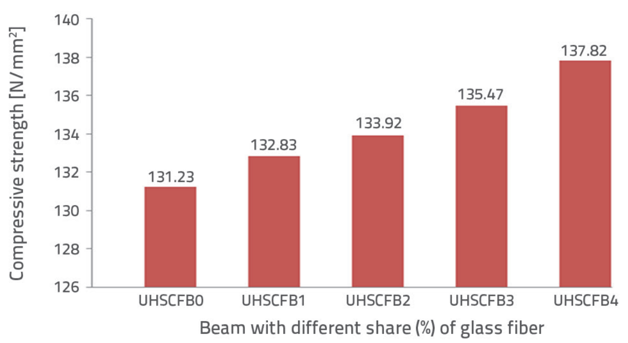


**Figure 3. Compressive strength of UHSC with different percentage of glass fiber, according to table 2**

### 5.2. Split tensile strength

The split tensile strength obtained in this study also increased with the gradual increase in fiber content up to an optimum percentage. In total, 15 cylinders with diameters of 150 mm and heights of 300 mm were cast and tested. The split tensile strength increased from 1 % to 2 % for every increment percentage of fiber content, as shown in Figure 4. Adding silica fume to other ingredients provides better mechanical properties [8].

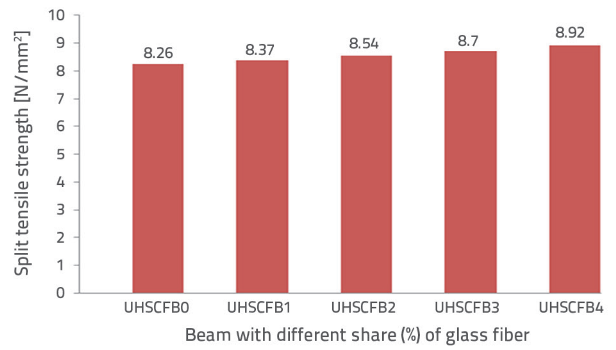


**Figure 4. Split tensile of UHSC with different percentage of glass fiber**

### 5.3. Flexural strength

Considering the flexural strength, 15 prisms of size 500 × 100 × 100 mm were cast and tested. The variation among the arrived mix without glass fiber and with glass fiber of 0.12 % was approximately 23 %, as shown in Figure 5, indicating an improvement in flexural behavior owing to the addition of fibers in concrete; the percentage variation of strength was higher than that of the compressive and split tensile strengths of the concrete. Fiber added UHSC specimens exhibit higher flexural strength than UHSC without fibers [3].

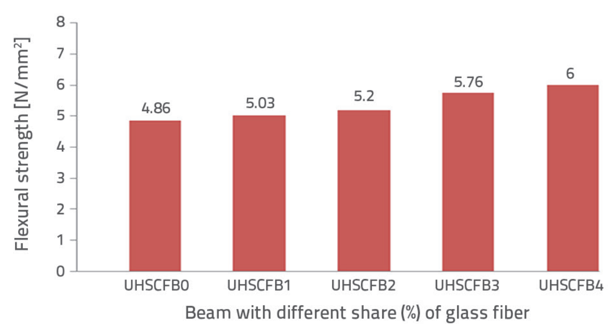


**Figure 5. Flexural strength of UHSC with different percentage of glass fiber, according to table 2**


**Figure 6. Experimental setup and testing of beams**

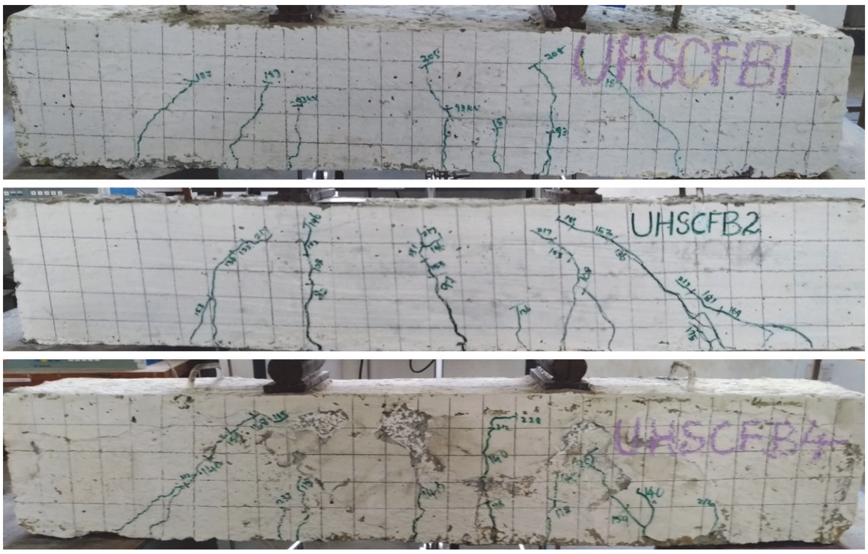


**Figure 7. Crack patterns in beams due to load**

### 5.4. Flexural and shear behavior of ultra-high strength glass fiber reinforced concrete beams

All the beams considered in this investigation were tested up to failure under symmetrically applied and gradually increasing two-point loads, as shown in Figure 6. There is an increase in ultimate load-carrying capacity of UHS-GFRC beam in flexural mode of failure (a/d = 2) at the optimum fiber content of 0.09 %. If the fiber content exceeds this limit, the load-carrying capacity also decreases; however, the ultimate load-carrying capacity attained is the maximum for the beam, comprising 0.12 % of glass fiber in the shear mode of failure (a/d = 1.6) because the load-carrying capacity of UHS-GFRC beams depends on the admixtures as well as the span to effective depth ratio. The crack patterns owing to the load are shown in Figure 7.

### 5.5. Load - Deflection relationships

The load was gradually applied over the beam using the setup above. The specifications of the first cracking load,

**Table 5. Details of experimental test results**

| S.No | Designation of beams | a/d | Cube strength of concrete [N/mm²] | First cracking load $W_{cr(E)}$ [kN] | Ultimate load $W_{u(E)}$ [kN] | Mode of Failure |
|---|---|---|---|---|---|---|
| ratio | UHSCFB0 | 2 | 131.23 | 105 | 119 | Flexure |
| 2 | UHSCSB0 | 1.6 | 131.23 | 71 | 147 | Shear |
| 3 | UHSCFB1 | 2 | 132.83 | 93 | 205 | Flexure |
| 4 | UHSCSB1 | 1.6 | 132.83 | 117 | 253 | Shear |
| 5 | UHSCFB2 | 2 | 133.92 | 82 | 217 | Flexure |
| 6 | UHSCSB2 | 1.6 | 133.92 | 126 | 301 | Shear |
| 7 | UHSCFB3 | 2 | 135.47 | 115 | 271 | Flexure |
| 8 | UHSCSB3 | 1.6 | 135.47 | 107 | 289 | Shear |
| 9 | UHSCFB4 | 2 | 137.82 | 118 | 248 | Flexure |
| 10 | UHSCSB4 | 1.6 | 137.82 | 105 | 266 | Shear |
| | | | | Mean | 256.25 | |
| | | | | Standard deviation | 33.02 | |
| | | | | Coefficient of variance | 12.88 % | |

ultimate load, and mode of failure are listed in Table 5. The load versus deflection curves owing to the shear and flexure modes of failure are shown in Figure 8. Three well-defined behaviors in the load-deflection relationship can be observed. In beam UHSCSB2, the line up to point A is linear and has a maximum slope. This corresponds to the pre- cracking stage. Cracking occurs at point A; hence, the slope of the graph changes. At point B, steel yielding occurs. Beyond point B, the graph is curvilinear, and the same is applicable for beam UHSCFB3. All other beams showed similar changes in the load-deflection graph.

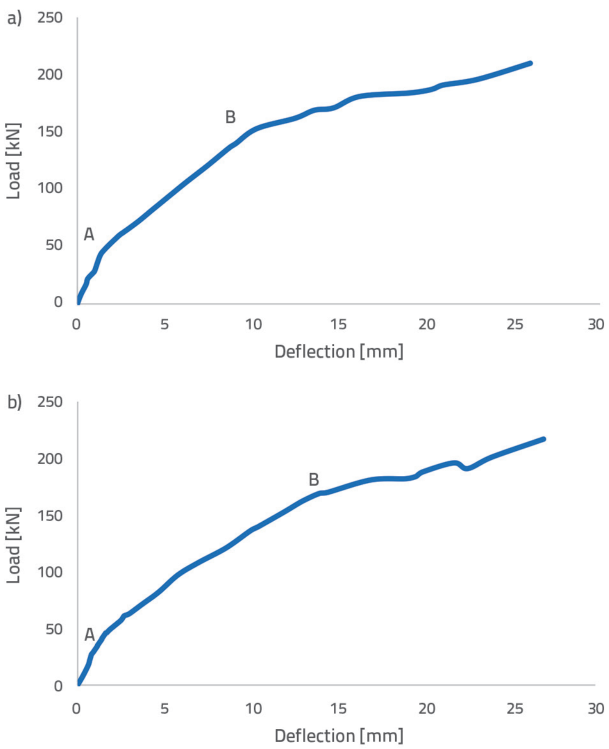


**Figure 8. Load versus deflection for shear mode of failure: a) UHSCSB2 Load – Deflection; b) UHSCFB3 Load – Deflection**

## 6. Conclusion

An investigation of UHSC is important to demonstrate various materials and combinations used for making UHSC, as well as an experiment detailing the flexural and shear behavior of UHS-GFRC beams for pre-cracking loads. Furthermore, graphs for load versus deflection for different percentages of glass fiber and span to effective depth ratio are necessary.

In this study, we investigated the flexural behavior of UHS-GFRC beams. Currently, no research article has been published on the flexural strength of these beams. This investigation led to the following conclusions:

- All the mixtures obtained in this study, with and without glass fiber, exhibited higher strength (compressive strength of more than 100 MPa).
- The UHSC RC beams tested with shear span to an effective depth ratio (av/d ratio) of 2.0 failed by flexural mode.
- The UHSC RC beams tested with a shear span to an effective depth ratio (av/d ratio) of 1.6 failed by shear mode.
- An increase in the glass fiber content up to an optimum percentage of 0.09 % by volume of concrete shows 24.88 % higher ultimate load-carrying capacity than 0.06 % fiber content and 8.48 % than 0.12 % fiber content in flexure mode of failure.
- An increase in the glass fiber content up to an optimum percentage of 0.06 % by volume of concrete shows 18.97 % higher ultimate load-carrying capacity than 0.03 % fiber content and 3.98 % than 0.09 % fiber content in the shear mode of failure.
- Irrespective of the percentage of glass fibers, the UHSC beams failed, owing to the initiation of yielding of the reinforcing steel and the subsequent crushing of concrete in the compression zone.
- The optimum percentage of glass fiber of 0.06 % to 0.12 % by volume of concrete with water- binder ratio of 0.2 and silica fume, superplasticizer, cement, M- sand, and coarse aggregate of size 12 mm is sufficient to produce an UHSC that can mix with better mechanical strength behavior. Furthermore, hollow beams with the same constituents can be developed to predict strength and behavior.

In future research, the application of non-destructive testing based on the application of piezoelectric smart aggregates, which enables active monitoring of the condition of structures and elements, should be considered, according to [14].

## Acknowledgements

The authors gratefully acknowledge the management of the Bannari Amman Institute of Technology, Erode for providing the laboratory facilities for conducting this investigation. The technical and experimental support provided by the teaching and laboratory technicians of the Bannari Amman Institute of Technology, Erode, is also acknowledged.

## REFERENCES

[1] Upendra Varma, A., Kumar, A.D.: Glass Fibre Reinforced Concrete, International Journal of Engineering Research and Applications, 3 (2013) 5.

[2] Md.Abid A., Imran, A., Fazlur, R.: Experimental Study on Properties of Glass Fibre Reinforced Concrete, International Journal of Engineering Trends and Technology (IJETT), 24 (2015) 6.

[3] Srinivas, A., Craig, M.N.: Ultra-High Strength Concrete Mixtures Using Local Materials, Journal of Civil Engineering and Architecture, 5 (2011).

[4] Magudeaswaran, P., Eswaramoorthi, P.: High Performance Concrete Using M Sand, Asian Journal of Research in Social Sciences and Humanities, 6 (2016), pp. 372-386.

[5] Vaitkevičius, V., Šerelis, E.: Influence of Silica Fume on Ultrahigh Performance Concrete, International Journal of Bioengineering and Life Sciences, 8 (2014).

[6] Venkatesan, G., Tamizhazhagan, T.: Ultra High Strength Concrete, International Journal of Innovative Research in Science, Engineering and Technology, 5 (2016).

[7] Sagura, R., Jagadeesan, R.: Experimental Study on Mechanical Properties of M-Sand Concrete by Different Curing Methods, IOSR Journal of Mechanical and Civil Engineering, e-ISSN: 2278-1684, p-ISSN: 2320-334X.

[8] Wu, Z., Shi, C., Khayat, K.H.: Influence of silica fume content on microstructure development and bond to steel fiber in ultra-high strength cement-based materials (UHSC), Cement and Concrete Composites, 2016.

[9] Choe, G., Kim, G., Nam, J., Kim, H., Hwang, E., Lee, S.: Effect of Mass Loss of Organic Fiber on the Water Vapor Pressure and Moisture Migration of 150 and 200 MPa Ultra-High Strength Concrete Exposed to High Temperature, Journal of Advanced Concrete Technology, 18 (2020), pp. 339-351.

[10] Zhang, G.Z., Cho, H.K., Wang, X.Y.: Effect of Nano-Silica on the Autogenous Shrinkage, Strength, and Hydration Heat of Ultra-High Strength Concrete, Applied sciences, 10 (2020).

[11] Shi, C., Wang, D., Wu, L., Wu, Z.: The hydration and microstructure of ultra-high strength concrete with cement - silica fume - slag binder, Cement and Concrete Composites, 61 (2015), pp. 44-52.

[12] Plank, J., Schroefl, C., Gruber, M., Lesti, M., Sieber, R.: Effectiveness of Polycarboxylate Superplasticizers in Ultra-High Strength Concrete: The importance of PCE Compatibility with Silica Fume, Journal of Advanced Concrete Technology, 7 (2009) 1, pp. 5-12.

[13] Bartosz, Z., Maciej, S., Pawet, O.: Ultra-high strength concrete made with recycled aggregate from sanitary ceramic wastes – The method of production and the interfacial transition zone; Construction and Building Materials, 122 (2016), pp. 736-742.

[14] Stojić, N., Nestorović, T., Stojić, D., Markovic, N., Stojković, N., Velimirović, N.: Energy based three-dimensional damage index for monitoring and damage detection of concrete structures, GRAĐEVINAR, 73 (2021) 12, pp. 1223-1238, https://doi.org/10.14256/JCE.2428.2018